

Low energy binding of composite dark matter with nuclei as a solution for the puzzles of dark matter searches

Maxim Yu. Khlopov^{1,2,3}, Andrey G. Mayorov¹, Evgeniy Yu. Soldatov¹

¹*Moscow Engineering Physics Institute (National Nuclear Research University), 115409 Moscow, Russia*

²*Centre for Cosmoparticle Physics "Cosmion" 115409 Moscow, Russia*

³*APC laboratory 10, rue Alice Domon et Léonie Duquet
75205 Paris Cedex 13, France*

Abstract

Positive results of dark matter searches in experiments DAMA/NaI and DAMA/LIBRA taken together with negative results of other groups can imply nontrivial particle physics solutions for cosmological dark matter. Stable particles with charge -2 bind with primordial helium in O-helium "atoms" (OHe), representing a specific Warmer than Cold nuclear-interacting form of dark matter. Slowed down in the terrestrial matter, OHe is elusive for direct methods of underground Dark matter detection like those used in CDMS experiment, but its low energy binding with nuclei can lead to annual variations of energy release in the interval of energy 2-6 keV in DAMA/NaI and DAMA/LIBRA experiments. Schrodinger equation for system of nucleus and OHe is considered and reduced to an equation of relative motion in a spherically symmetrical potential, formed by the Yukawa tail of nuclear scalar isoscalar attraction potential, acting on He beyond the nucleus, and dipole Coulomb repulsion between the nucleus and OHe at distances from the nuclear surface, smaller than the size of OHe. The values of coupling strength and mass of meson, mediating scalar isoscalar nuclear potential, are rather uncertain. Within these uncertainties and in the approximation of rectangular potential wells we find a range of these parameters, at which the sodium and/or iodine nuclei have a few keV binding energy with OHe. At nuclear parameters, reproducing DAMA results, the energy release predicted for detectors with chemical content other than NaI differ in the most cases from the one in DAMA detector. In particular, it is shown that in the case of CDMS germanium state has binding energy with OHe beyond the range of 2-6 keV and its formation should not lead to ionization in the energy range of DAMA signal. Due to dipole Coulomb barrier, transitions to more energetic levels of Na(I)+OHe system with much higher energy release are suppressed in the correspondence with the results of DAMA experiments. The proposed explanation inevitably leads to prediction of abundance of anomalous Na and I, corresponding to the signal, observed by DAMA.

1 Introduction

The widely shared belief is that the dark matter, corresponding to 25% of the total cosmological density, is nonbaryonic and consists of new stable particles. One can formulate the set of conditions under which new particles can be considered as candidates to dark matter (see e.g. [1, 2, 3] for review and reference): they should be stable, saturate the measured dark matter density and decouple from plasma and radiation at least before the beginning of matter dominated stage. The easiest way to satisfy these conditions is to involve neutral weakly interacting particles. However it is not the only particle physics solution for the dark matter problem. In the composite dark matter scenarios new stable particles can have electric charge, but escape experimental discovery, because they are hidden in atom-like states maintaining dark matter of the modern Universe.

It offers new solutions for the physical nature of the cosmological dark matter. The main problem for these solutions is to suppress the abundance of positively charged species bound with ordinary electrons, which behave as anomalous isotopes of hydrogen or helium. This problem is unresolvable, if the model predicts stable particles with charge -1, as it is the case for tera-electrons [4, 5]. To avoid anomalous isotopes overproduction, stable particles with charge -1 should be absent, so that stable negatively charged particles should have charge -2 only.

Elementary particle frames for heavy stable -2 charged species are provided by: (a) stable "antibaryons" $\bar{U}\bar{U}\bar{U}$ formed by anti- U quark of fourth generation [6, 7, 8, 9] (b) AC-leptons [8, 10, 11], predicted in the extension [10] of standard model, based on the approach of almost-commutative geometry [12]. (c) Technileptons and anti-technibaryons [13] in the framework of walking technicolor models (WTC) [14]. (d) Finally, stable charged clusters $\bar{u}_5\bar{u}_5\bar{u}_5$ of (anti)quarks \bar{u}_5 of 5th family can follow from the approach, unifying spins and charges [15].

In the asymmetric case, corresponding to excess of -2 charge species, X^{--} , as it was assumed for $(\bar{U}\bar{U}\bar{U})^{--}$ in the model of stable U -quark of a 4th generation, as well as can take place for $(\bar{u}_5\bar{u}_5\bar{u}_5)^{--}$ in the approach [15] their positively charged partners effectively annihilate in the early Universe. Such an asymmetric case was realized in [13] in the framework of WTC, where it was possible to find a relationship between the excess of negatively charged anti-techni-baryons $(\bar{U}\bar{U})^{--}$ and/or technileptons ζ^{--} and the baryon asymmetry of the Universe. The relationship between baryon asymmetry and excess of -2 charge stable species is supported by sphaleron transitions at high temperatures and can be realized in all the models, in which new stable species belong to non-trivial representations of electroweak $SU(2)$ group.

After it is formed in the Standard Big Bang Nucleosynthesis (SBBN), ${}^4\text{He}$ screens the X^{--} charged particles in composite (${}^4\text{He}^{++}X^{--}$) *O-helium* “atoms” [6]. For different models of X^{--} these “atoms” are also called ANO-helium [7, 8], Ole-helium [8, 11] or techni-O-helium [13]. We’ll call them all O-helium (*OHe*) in our further discussion, which follows the guidelines of [16].

In all these forms of O-helium X^{--} behave either as leptons or as specific “heavy quark clusters” with strongly suppressed hadronic interaction. Therefore O-helium interaction with matter is determined by nuclear interaction of *He*. These neutral primordial nuclear interacting objects contribute to the modern dark matter density and play the role of a nontrivial form of strongly interacting dark matter [17, 18]. The active influence of this type of dark matter on nuclear transformations seems to be incompatible with the expected dark matter properties. However, it turns out that the considered scenario of nuclear-interacting O-helium Warmer than Cold Dark Matter is not easily ruled out [6, 11, 13, 19] and challenges the experimental search for various forms of O-helium and its charged constituents.

Here we concentrate on its effects in underground detectors. We present qualitative confirmation of the earlier guess [16, 20] that the positive results of dark matter searches in DAMA/NaI (see for review [21]) and DAMA/LIBRA [22] experiments can be explained by O-helium, resolving the controversy between these results and negative results of other experimental groups.

2 OHe in the terrestrial matter

The evident consequence of the O-helium dark matter is its inevitable presence in the terrestrial matter, which appears opaque to O-helium and stores all its in-falling flux.

After they fall down terrestrial surface, the in-falling *OHe* particles are effectively slowed down due to elastic collisions with matter. Then they drift, sinking down towards the center of the Earth with velocity

$$V = \frac{g}{n\sigma v} \approx 80S_3A^{1/2} \text{ cm/s}. \quad (1)$$

Here $A \sim 30$ is the average atomic weight in terrestrial surface matter, $n = 2.4 \cdot 10^{24}/A \text{ cm}^{-3}$ is the number density of terrestrial atomic nuclei, σv is the rate of nuclear collisions, $m_o \approx M_X + 4m_p = S_3 \text{ TeV}$ is the mass of O-helium, M_X is the mass of the X^{--} component of O-helium, m_p is the mass of proton and $g = 980 \text{ cm/s}^2$.

Near the Earth’s surface, the O-helium abundance is determined by the equilibrium between the in-falling and down-drifting fluxes.

The in-falling O-helium flux from dark matter halo is

$$F = \frac{n_0}{8\pi} \cdot |\overline{V}_h + \overline{V}_E|,$$

where V_h -speed of Solar System (220 km/s), V_E -speed of Earth (29.5 km/s) and $n_0 = 3 \cdot 10^{-4} S_3^{-1} \text{ cm}^{-3}$ is the local density of O-helium dark matter. For qualitative estimation we don't take into account here velocity dispersion and distribution of particles in the incoming flux that can lead to significant effect.

At a depth L below the Earth's surface, the drift timescale is $t_{dr} \sim L/V$, where $V \sim 400 S_3 \text{ cm/s}$ is given by Eq. (1). It means that the change of the incoming flux, caused by the motion of the Earth along its orbit, should lead at the depth $L \sim 10^5 \text{ cm}$ to the corresponding change in the equilibrium underground concentration of OHe on the timescale $t_{dr} \approx 2.5 \cdot 10^2 S_3^{-1} \text{ s}$.

The equilibrium concentration, which is established in the matter of underground detectors at this timescale, is given by

$$n_{oE} = \frac{2\pi \cdot F}{V} = n_0 \frac{n\sigma v}{4g} \cdot |\overline{V}_h + \overline{V}_E|, \quad (2)$$

where, with account for $V_h > V_E$, relative velocity can be expressed as

$$\begin{aligned} |\overline{V}_o| &= \sqrt{(\overline{V}_h + \overline{V}_E)^2} = \sqrt{V_h^2 + V_E^2 + V_h V_E \sin(\theta)} \simeq \\ &\simeq V_h \sqrt{1 + \frac{V_E}{V_h} \sin(\theta)} \sim V_h \left(1 + \frac{1}{2} \frac{V_E}{V_h} \sin(\theta)\right). \end{aligned}$$

Here $\theta = \omega(t - t_0)$ with $\omega = 2\pi/T$, $T = 1yr$ and t_0 is the phase. Then the concentration takes the form

$$n_{oE} = n_{oE}^{(1)} + n_{oE}^{(2)} \cdot \sin(\omega(t - t_0)) \quad (3)$$

So, there are two parts of the signal: constant and annual modulation, as it is expected in the strategy of dark matter search in DAMA experiment [22].

Such neutral (${}^4He^{++}X^{--}$) "atoms" may provide a catalysis of cold nuclear reactions in ordinary matter (much more effectively than muon catalysis). This effect needs a special and thorough investigation. On the other hand, X^{--} capture by nuclei, heavier than helium, can lead to production of anomalous isotopes, but the arguments, presented in [6, 11, 13] indicate that their abundance should be below the experimental upper limits.

It should be noted that the nuclear cross section of the O-helium interaction with matter escapes the severe constraints [18] on strongly interacting

dark matter particles (SIMPs) [17, 18] imposed by the XQC experiment [23]. Therefore, a special strategy of direct O-helium search is needed, as it was proposed in [24].

In underground detectors, *OHe* “atoms” are slowed down to thermal energies and give rise to energy transfer $\sim 2.5 \cdot 10^{-4} \text{ eVA}/S_3$, far below the threshold for direct dark matter detection. It makes this form of dark matter insensitive to the severe CDMS constraints [25]. However, *OHe* induced processes in the matter of underground detectors can result in observable effects.

3 Low energy bound state of O-helium with nuclei

In the essence, our explanation of the results of experiments DAMA/NaI and DAMA/LIBRA is based on the idea that OHe, slowed down in the terrestrial matter and present in the matter of DAMA detectors, can form a few keV bound state with nucleus, in which OHe is situated **beyond** the nucleus. Formation of such bound state leads to the corresponding energy release and ionization signal, detected in DAMA experiments.

3.1 Low energy bound state of O-helium with nuclei

We assume the following picture: at the distances larger, than its size, OHe is neutral and it feels only Yukawa exponential tail of nuclear attraction, due to scalar-isoscalar nuclear potential. It should be noted that scalar-isoscalar nature of He nucleus excludes its nuclear interaction due to π or ρ meson exchange, so that the main role in its nuclear interaction outside the nucleus plays σ meson exchange, on which nuclear physics data are not very definite. When the distance from the surface of nucleus becomes smaller than the size of OHe, the mutual attraction of nucleus and OHe is changed by dipole Coulomb repulsion. Inside the nucleus strong nuclear attraction takes place. In the result the spherically symmetric potential appears, given by

$$U = -\frac{A_{He}A g^2 \exp(-\mu r)}{r} + \frac{Z_{He}Z e^2 r_o \cdot F(r)}{r^2}. \quad (4)$$

Here $A_{He} = 4$, $Z_{He} = 2$ are atomic weight and charge of helium, A and Z are respectively atomic weight and charge of nucleus, μ and g^2 are the mass and coupling of scalar-isoscalar meson - mediator of nuclear attraction, r_o is the size of OHe and $F(r)$ is its electromagnetic formfactor, which strongly suppresses the strength of dipole electromagnetic interaction outside the OHe “atom”.

Schrodinger equation for this system is reduced (taking apart the equation for the center of mass) to the equation of relative motion for the reduced mass

$$m = \frac{Am_p m_o}{Am_p + m_o}, \quad (5)$$

where m_p is the mass of proton.

In the case of orbital momentum $l=0$ the wave functions depend only on r .

To simplify the solution of Schrodinger equation we approximate the potential (4) by a rectangular potential that consists of a deep potential well within the radius of nucleus R_A , of a rectangular dipole Coulomb potential barrier outside its surface up to the radial layer $a = R_A + r_o$, where it is suppressed by the OHe atom formfactor, and of the outer potential well of the width $\sim 1/\mu$, formed by the tail of Yukawa nuclear interaction. It leads to the approximate potential, given by

$$\left\{ \begin{array}{l} r < R_A : U = U_1 = -\frac{4Ag^2 \exp(-\mu R_A)}{R_A}, \\ R_A < r < a : U = U_2 = \frac{\int_{R_A}^{R_A+r_o} \frac{2Z\alpha 4\pi(r_o/x)}{x} dx}{r_o}, \\ a < r < b : U = U_3 = \frac{4Ag^2 \exp(-\mu(R_A + r_o))}{R_A + r_o}, \\ b < r : U = U_4 = 0, \end{array} \right. \quad (6)$$

presented on Fig. 1.

Solutions of Schrodinger equation for each of the four regions, indicated on Fig. 1, are considered in Appendix. In the result of their sewing one obtains the condition for the existence of a low-energy level in OHe-nucleus system,

$$\sin(k_3 b + \delta) = \sqrt{\frac{1}{2mU_3}} \cdot k_3, \quad (7)$$

where k_3 and δ are, respectively, the wave number and phase of the wave function in the region III (see Appendix for details).

With the use of the potential (6) in the Eq.(7), intersection of the two lines gives graphical solution presented on Fig. 2.

Based on this solution one obtains from Eq.(22) the energy levels of a bound state in the considered potential well.

The energy of this bound state and its existence strongly depend on the parameters μ and g^2 of nuclear potential (4). On the Fig. 3 the region of these parameters, giving 2-6 keV energy level in OHe bound states with sodium and iodine are presented. In these calculations the mass of OHe was taken equal to $m_o = 1TeV$.

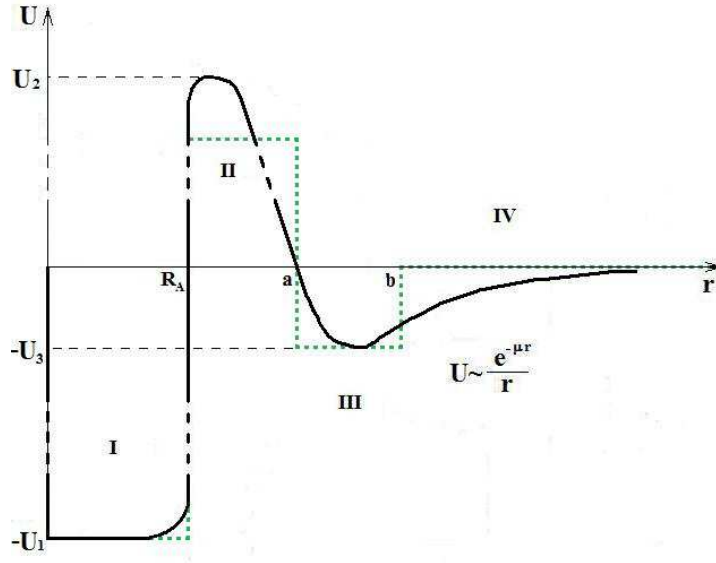


Figure 1: The approximation of rectangular well for potential of OHe-nucleus system.

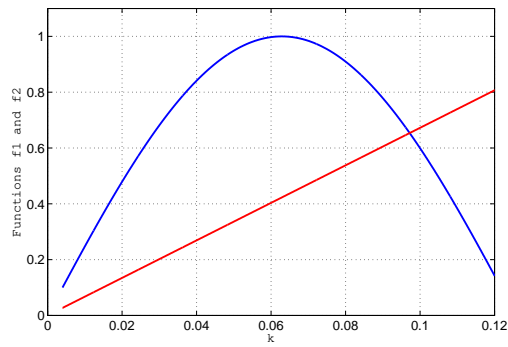


Figure 2: Graphical solution of transcendental equation.

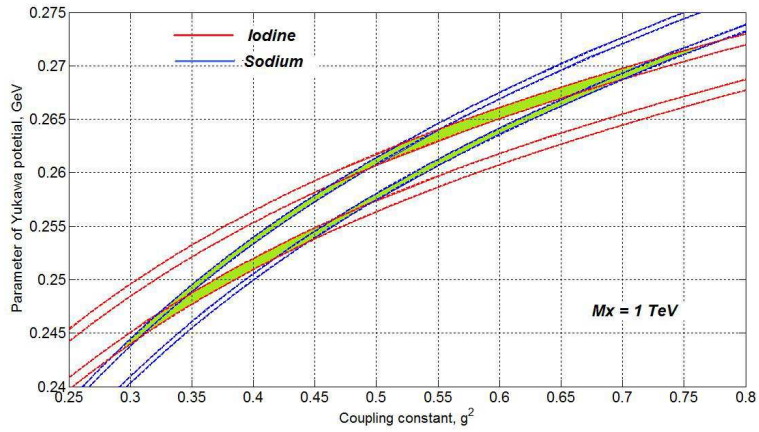


Figure 3: The region of parameters μ and g^2 , for which Na and I have a level in the interval 2-6 keV. For each nucleus two narrow strips determine the region of parameters, at which the bound system of this element with OHe has a level in 2-6 keV energy range. The outer line of strip corresponds to the level of 6 keV and the internal line to the level of 2 keV. The region of intersection of strips correspond to existence of 2-6 keV levels in both OHe-Na and OHe-I systems, while the piece of strip between strips of other nucleus corresponds to the case, when OHe bound state with this nucleus has 2-6 keV level, while the binding energy of OHe with the other nuclei is less than 2 keV by absolute value.

The rate of radiative capture of OHe by nuclei should be accurately calculated with the use of exact form of wave functions, obtained for the OHe-nucleus bound state. This work is now in progress. One can use the analogy with the radiative capture of neutron by proton, considered in textbooks (see e.g. [26]) with the following corrections:

- There is only E1 transition in the case of OHe capture.
- The reduced masses of n-p and OHe-nucleus systems are different
- The existence of dipole Coulomb barrier leads to a suppression of the cross section of OHe radiative capture.

With the account for these effects our first estimations give the rate of OHe radiative capture, reproducing the level of signal, detected by DAMA.

Formation of OHe-nucleus bound system leads to energy release of its binding energy, detected as ionization signal in DAMA experiment. In the context of our approach the existence of annual modulations of this signal in the range 2-6 keV and absence of such effect at energies above 6 keV means that binding energy of Na-OHe and I-OHe systems should not exceed 6 keV, being in the range 2-6 keV for at least one of these elements. These conditions were taken into account for determination of nuclear parameters, at which the result of DAMA can be reproduced. At these values of μ and g^2 energy of OHe binding with other nuclei can strongly differ from 2-6 keV. In particular, energy release at the formation of OHe bound state with thallium can be larger than 6 keV. However, taking into account that thallium content in DAMA detector is 3 orders of magnitude smaller, than NaI, such signal is to be below the experimental errors.

It should be noted that the results of DAMA experiment exhibit also absence of annual modulations at the energy of MeV-tens MeV. Energy release in this range should take place, if OHe-nucleus system comes to the deep level inside the nucleus (in the region I of Fig. 1). This transition implies tunneling through dipole Coulomb barrier and is suppressed below the experimental limits.

3.2 Energy levels in other nuclei

For the chosen range of nuclear parameters, reproducing the results of DAMA/NaI and DAMA/LIBRA, we can calculate the binding energy of OHe-nucleus states in nuclei, corresponding to chemical composition of set-ups in other experiments. The results of such calculation for germanium, corresponding to the detector of CDMS experiment, are presented on Fig. 4. For all the parameters, reproducing results of DAMA experiment the predicted energy level of OHe-germanium bound state is beyond the range

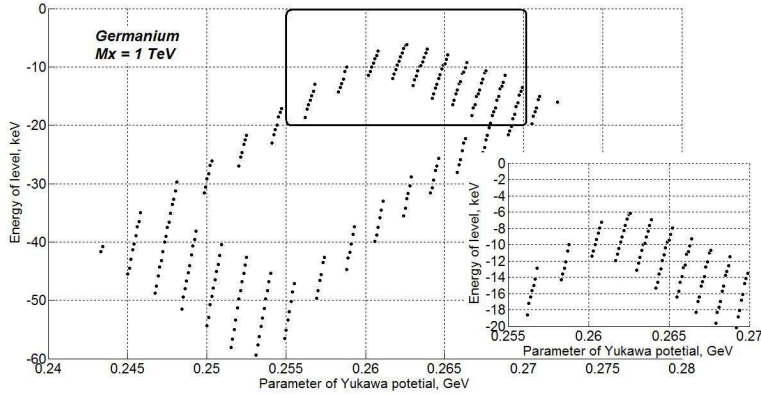


Figure 4: Energy levels in OHe bound system with germanium. The range of energies close to energy release in DAMA experiment is blown up to demonstrate that even in this range there is no formal intersection with DAMA results.

2-6 keV, being dominantly in the range of tens - few-tens keV by absolute value. It makes elusive a possibility to test DAMA results by search for ionization signal in the same range 2-6 keV in other set-ups with content that differs from Na and I. In particular, our approach naturally predicts absence of ionization signal in the range 2-6 keV in accordance with the recent results of CDMS [27].

We have also calculated the energies of bound states of OHe with xenon (Fig. 5), argon (Fig. 6), carbon (Fig. 7), aluminium (Fig. 8), fluorine (Fig. 9), chlorine (Fig. 10) and oxygen (Fig. 11).

3.3 Superheavy OHe

In view of possible applications for the approach, unifying spins and charges [15], we consider here the case of superheavy OHe, since the candidate for X^{--} , coming from stable 5th generation ($\bar{u}_5\bar{u}_5\bar{u}_5$) is probably much heavier, than 1 TeV. With the growth of the mass of O-helium the reduced mass (5) slightly grows, approaching with higher accuracy the mass of nucleus. It extends a bit the range of nuclear parameters μ and g^2 , at which the binding energy of OHe with sodium and/or iodine is within the range 2-6 keV (see Fig. 12). At these parameters the binding energy of O-helium with germanium and xenon are presented on figures 13 and 14, respectively. Qualitatively, these predictions are similar to the case of $S_3 = 1$. Though there appears a narrow window with OHe-Ge binding energy, below 6 keV for the dominant range of parameters energy release in CDMS is predicted

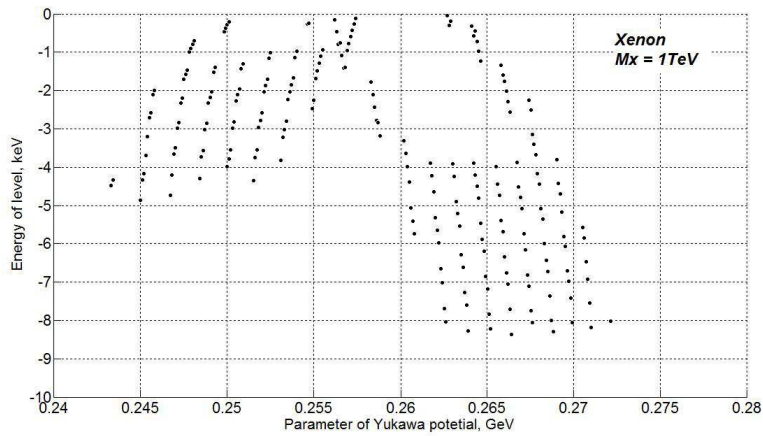


Figure 5: Energy levels in OHe bound system with xenon.

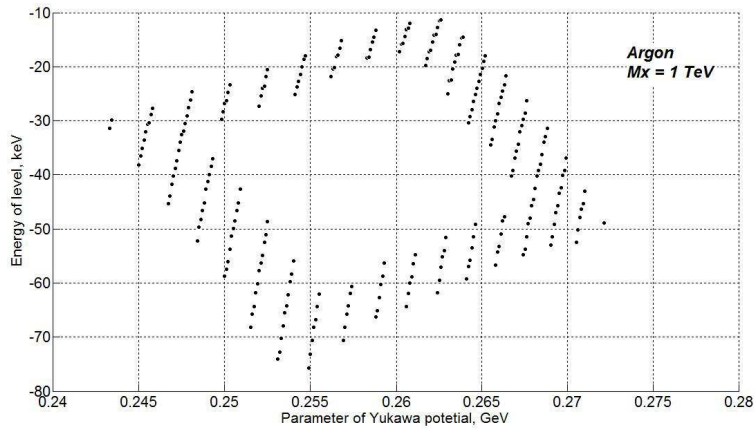


Figure 6: Energy levels in OHe bound system with argon.

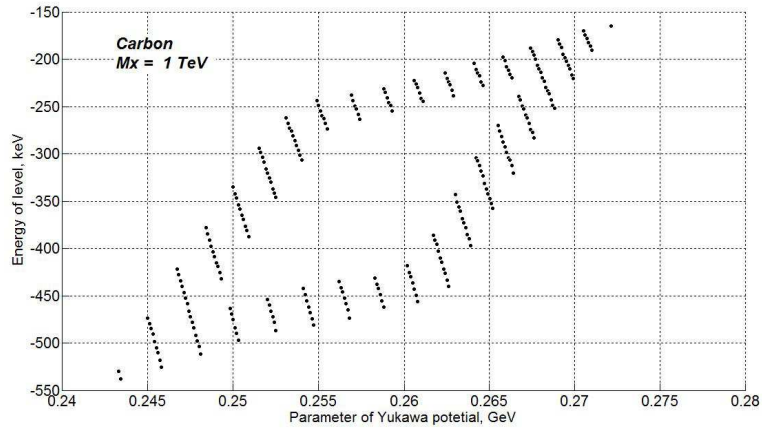


Figure 7: Energy levels in OHe bound system with carbon.

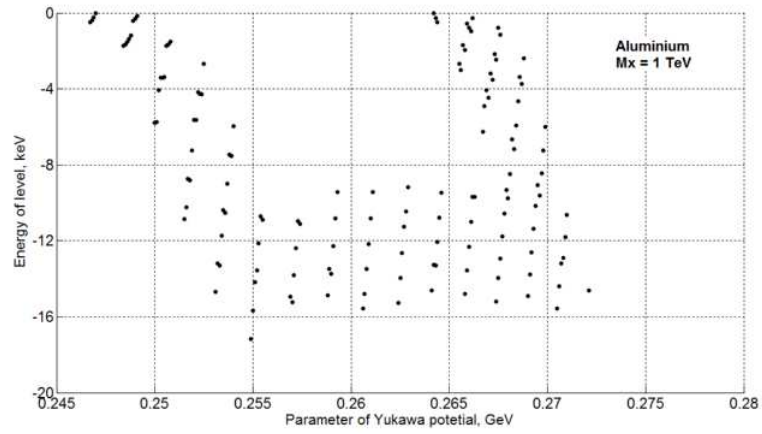


Figure 8: Energy levels in OHe bound system with aluminium.

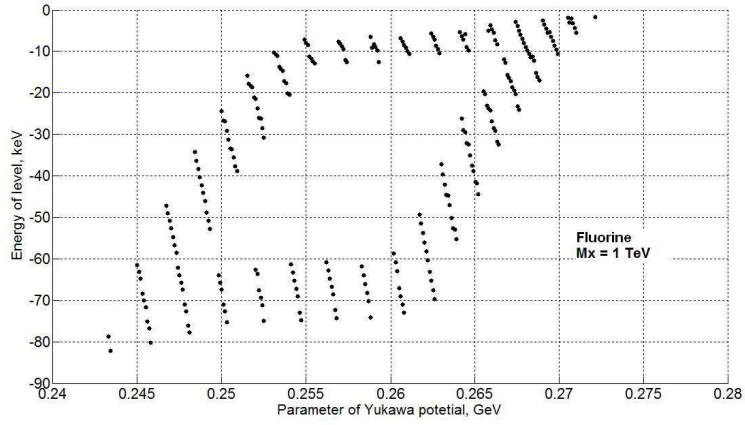


Figure 9: Energy levels in OHe bound system with fluorine.

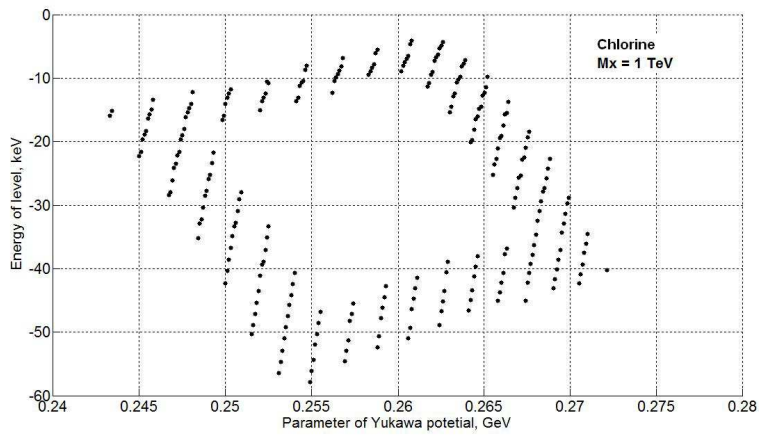


Figure 10: Energy levels in OHe bound system with chlorine.

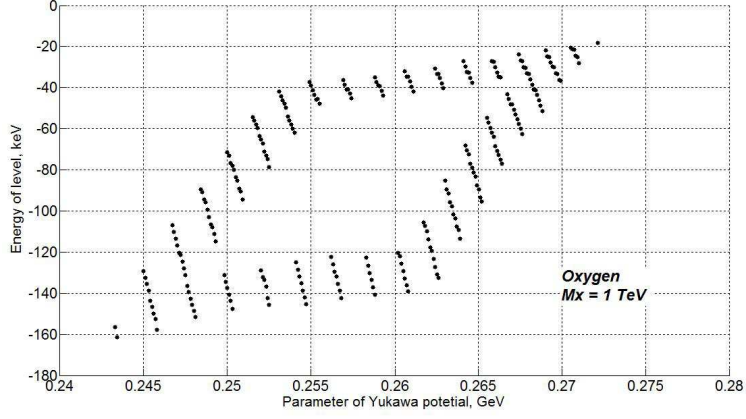


Figure 11: Energy levels in OHe bound system with oxygen.

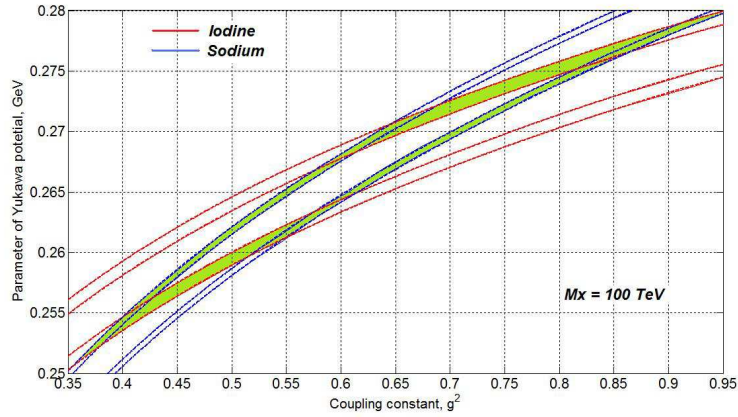


Figure 12: The range of parameters μ and g^2 , for which Na and I have a level in the interval 2-6 keV for $S_3 = 100$. This range becomes a bit wider as compared with the case of $S_3 = 1$, presented on Fig. 3.

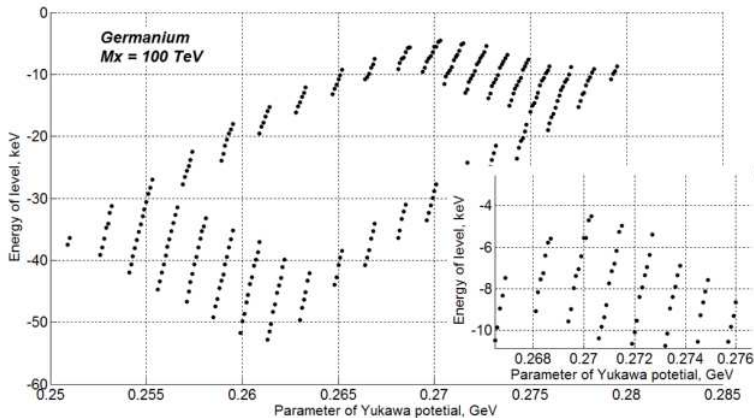


Figure 13: Energy levels in OHe bound system with germanium.

to be of the order of few tens keV.

4 Conclusions

To conclude, the results of dark matter search in experiments DAMA/NaI and DAMA/LIBRA can be explained in the framework of composite dark matter scenario without contradiction with negative results of other groups. This scenario can be realized in different frameworks, in particular in Minimal Walking Technicolor model or in the approach unifying spin and charges and contains distinct features, by which the present explanation can be distinguished from other recent approaches to this problem [28] (see also review and more references in [29]).

Our explanation is based on the mechanism of low energy binding of OHe with nuclei. We have found that within the uncertainty of nuclear physics parameters there exists a range at which OHe binding energy with sodium and/or iodine is in the interval 2-6 keV. Radiative capture of OHe to this bound state leads to the corresponding energy release observed as an ionization signal in DAMA detector.

OHe concentration in the matter of underground detectors is determined by the equilibrium between the incoming cosmic flux of OHe and diffusion towards the center of Earth. It is rapidly adjusted and follows the change in this flux with the relaxation time of few minutes. Therefore the rate of radiative capture of OHe should experience annual modulations reflected in annual modulations of the ionization signal from these reactions.

An inevitable consequence of the proposed explanation is appearance

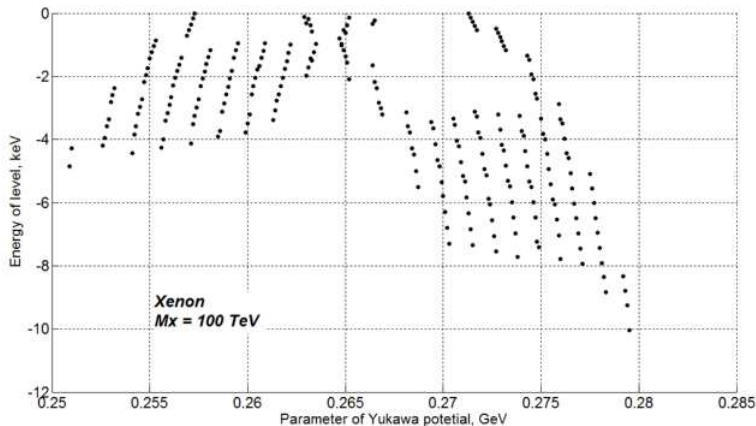


Figure 14: Energy levels in OHe bound system with xenon.

in the matter of DAMA/NaI or DAMA/LIBRA detector anomalous superheavy isotopes of sodium and/or iodine, having the mass roughly by m_o larger, than ordinary isotopes of these elements. If the atoms of these anomalous isotopes are not completely ionized, their mobility is determined by atomic cross sections and becomes about 9 orders of magnitude smaller, than for O-helium. It provides their conservation in the matter of detector. Therefore mass-spectroscopic analysis of this matter can provide additional test for the O-helium nature of DAMA signal. Methods of such analysis should take into account the fragile nature of OHe-Na (and/or OHe-I) bound states. Their binding energy is only few keV.

With the account for high sensitivity of our results to the values of uncertain nuclear parameters and for the approximations, made in our calculations, the presented results can be considered only as an illustration of the possibility to explain puzzles of dark matter search in the framework of composite dark matter scenario. However, even at the present level of our studies we can make a conclusion that the ionization signal expected in detectors with the content, different from NaI, can be dominantly in the energy range beyond 2-6 keV. Therefore test of results of DAMA/NaI and DAMA/LIBRA experiments by other experimental groups can become a very nontrivial task.

5 Acknowledgments

We would like to thank Jean Pierre Gazeau for discussions.

Appendix. Solution of Schrodinger equation for rectangular well

In the 4 regions, indicated on Fig. 1, Schrodinger equation has the form

$$I : \frac{1}{r} \frac{d^2}{dr^2}(r\psi_1) + k_1(r)^2\psi_1 = 0, k_1(r) = k_1 = \sqrt{2m(U_1 - |E|)}; \quad (8)$$

$$II : \frac{1}{r} \frac{d^2}{dr^2}(r\psi_2) + k_2(r)^2\psi_2 = 0, k_2(r) = k_2 = \sqrt{2m(U_2 - |E|)}; \quad (9)$$

$$III : \frac{1}{r} \frac{d^2}{dr^2}(r\psi_3) + k_3(r)^2\psi_3 = 0, k_3(r) = k_3 = \sqrt{2m(U_3 - |E|)}; \quad (10)$$

$$IV : \frac{1}{r} \frac{d^2}{dr^2}(r\psi_4) - k_4(r)^2\psi_4 = 0, k_4(r) = k_4 = \sqrt{2m|E|}. \quad (11)$$

The wave functions in these regions with the account for the boundary conditions have the form [30]

$$I : \psi_1 = A \frac{\sin(k_1 r)}{r}; \quad (12)$$

$$II : \psi_2 = \frac{B_1 \cdot \exp(-k_2 r) + B_2 \cdot \exp(k_2 r)}{r}; \quad (13)$$

$$III : \psi_3 = C \frac{\sin(k_3 r + \delta)}{r} \quad (14)$$

$$IV : \psi_4 = D \frac{\exp(-k_4 r)}{r} \quad (15)$$

The conditions of continuity of a logarithmic derivative $\frac{\psi'_i}{\psi_i} = \frac{\psi'_{i+1}}{\psi_{i+1}}$ $r\psi$ at the boundaries of these regions $r = R_A$, $r = a$ and $r = b$ are given by

$$I - II : k_1 \cdot \text{ctg}(k_1 R_A) = k_2 \cdot \frac{\exp(k_2 R_A) - F \cdot \exp(-k_2 R_A)}{\exp(k_2 R_A) + F \cdot \exp(-k_2 R_A)}, \quad (16)$$

$$II - III : k_3 \cdot \text{ctg}(k_3 a + \delta) = k_2 \cdot \frac{\exp(k_2 a) - F \cdot \exp(-k_2 a)}{\exp(k_2 a) + F \cdot \exp(-k_2 a)}, \quad (17)$$

$$III - IV : k_3 \cdot \text{ctg}(k_3 b + \delta) = -k_4, \quad (18)$$

where

$$F = B_1/B_2. \quad (19)$$

Now we can solve this system of equations for 3 variables. It follows from Eq. (16) that

$$F = \exp(2k_2 R_A) \cdot \frac{k_2 - k_1 \cdot \text{ctg}(k_1 R_A)}{k_2 + k_1 \cdot \text{ctg}(k_1 R_A)}, \quad (20)$$

and from Eq. (17)

$$\delta = -k_3 a + \text{arccctg}\left(\frac{k_2}{k_3} \cdot \frac{\exp(k_2 a) - F \cdot \exp(-k_2 a)}{\exp(k_2 a) + F \cdot \exp(-k_2 a)}\right). \quad (21)$$

Since

$$E = U(r) - \frac{k^2}{2m}, \quad (22)$$

one has

$$k_4 = \sqrt{2mU - k_3^2}, \quad (23)$$

Then Eq.(18) has the form

$$k_3^2 \left[\frac{1}{\sin^2(k_3 b + \delta)} - 1 \right] = 2mU_3 - k_3^2, \quad (24)$$

References

- [1] M.Yu. Khlopov *Cosmoparticle physics* (World Scientific, Singapore, 1999).
- [2] M.Yu. Khlopov in *Cosmion-94*, Eds. M.Yu.Khlopov et al. (Editions frontieres, 1996) P. 67; M. Y. Khlopov in hep-ph/0612250 , p 51.
- [3] M. Y. Khlopov in arXiv:0711.4681, p. 114; M. Y. Khlopov and N. S. Mankoc-Borstnik, *ibid*, p. 195.
- [4] S. L. Glashow, arXiv:hep-ph/0504287.
- [5] D. Fargion and M. Khlopov, arXiv:hep-ph/0507087.
- [6] M.Yu. Khlopov, *JETP Lett.* **83**, 1 (2006).
- [7] K. Belotsky *et al*, arXiv:astro-ph/0602261. K. Belotsky *et al*, *Gravitation and Cosmology* **12**, 1 (2006); K. Belotsky *et al*, arXiv:0806.1067 [astro-ph].

- [8] M. Y. Khlopov, arXiv:astro-ph/0607048.
- [9] K.M.Belotsky *et al*, *Gravitation and Cosmology* **11**, 3 (2005)
- [10] C. A. Stephan, arXiv:hep-th/0509213.
- [11] D. Fargion *et al*, *Class. Quantum Grav.* **23**, 7305 (2006); M. Y. Khlopov and C. A. Stephan, arXiv:astro-ph/0603187.
- [12] A. Connes *Noncommutative Geometry* (Academic Press, London and San Diego, 1994).
M. Y. Khlopov and C. A. Stephan, arXiv:astro-ph/0603187.
- [13] M. Y. Khlopov and C. Kouvaris, *Phys. Rev. D* **77**, 065002 (2008).
- [14] F. Sannino and K. Tuominen, *Phys. Rev. D* **71**, 051901 (2005); D. K. Hong *et al*, *Phys. Lett. B* **597**, 89 (2004); D. D. Dietrich *et al*, *Phys. Rev. D* **72**, 055001 (2005); D. D. Dietrich *et al*, arXiv:hep-ph/0510217; S. B. Gudnason *et al*, *Phys. Rev. D* **73**, 115003 (2006); S. B. Gudnason *et al*, *Phys. Rev. D* **74**, 095008 (2006).
- [15] N.S. Mankoč Borštnik, This Volume; A. Borštnik Bračič, N.S. Mankoč Borštnik, *Phys. Rev. D* **74**, 073013 (2006); N.S. Mankoč Borštnik, *Mod. Phys. Lett. A* **10**, 587 (1995); N.S. Mankoč Borštnik, *Int. J. Theor. Phys.* **40**, 315 (2001); G. Bregar, M. Breskvar, D. Lukman, N.S. Mankoč Borštnik, *New J. of Phys.* **10**, 093002 (2008).
- [16] M. Y. Khlopov, arXiv:0806.3581 [astro-ph].
- [17] C.B. Dover *et al*, *Phys. Rev. Lett.* **42**, 1117 (1979); S. Wolfram, *Phys. Lett. B* **82**, 65 (1979); G.D. Starkman *et al*, *Phys. Rev. D* **41**, 3594 (1990); D. Javorsek *et al*, *Phys. Rev. Lett.* **87**, 231804 (2001); S. Mitra, *Phys. Rev. D* **70**, 103517 (2004); G. D. Mack *et al*, *Phys. Rev. D* **76**, 043523 (2007);
- [18] B.D. Wandelt *et al.*, arXiv:astro-ph/0006344; P. C. McGuire and P. J. Steinhardt, arXiv:astro-ph/0105567; G. Zaharijas and G.R. Farrar, *Phys. Rev. D* **72**, 083502 (2005)
- [19] M. Y. Khlopov, arXiv:0801.0167 [astro-ph]; M. Y. Khlopov, arXiv:0801.0169 [astro-ph].
- [20] M. Y. Khlopov and C. Kouvaris, *Phys. Rev. D* **78**, 065040 (2008)
- [21] R. Bernabei *et al.*, *Rivista Nuovo Cimento* **26**, 1 (2003)

- [22] R. Bernabei *et al.* [DAMA Collaboration], *Eur.Phys.J C* **56**, 333 (2008) arXiv:0804.2741 [astro-ph].
- [23] D. McCammon *et al.*, *Nucl. Instrum. Methods A* **370**, 266 (1996); D. McCammon *et al.*, *Astrophys. J.* **576**, 188 (2002).
- [24] K. Belotsky *et al.*, arXiv:astro-ph/0606350.
- [25] D. S. Akerib *et al.* [CDMS Collaboration], *Phys. Rev. Lett.* **96**, 011302 (2006); Z. Ahmed *et al.* [CDMS Collaboration], arXiv:0802.3530 [astro-ph].
N. Mirabolfathi *et al.* [CDMS Collaboration], *Nucl. Instrum. Methods A* **559**, 417 (2006);
- [26] V. B. Berestecky, E. M. Lifshitz, L. P. Pitaevsky *Quantum Electrodynamics* (Nauka, Moscow, 1989).
- [27] O. Kamaev, for the CDMS Collaboration, arXiv:0910.3005 [hep-ex].
- [28] F. Petriello and K. M. Zurek, *JHEP* **0809**, 047 (2008); R. Foot, *Phys. Rev. D* **78**, 043529 (2008); J. L. Feng, J. Kumar and L. E. Strigari, arXiv:0806.3746 [hep-ph]; J. L. Feng, J. Kumar, J. Learned and L. E. Strigari, arXiv:0808.4151 [hep-ph]; E. M. Drobyshevski, arXiv:0811.0151 [astro-ph].
- [29] G. B. Gelmini, arXiv:0810.3733 [hep-ph].
- [30] L. D. Landau, E. M. Lifshitz *Quantum Mechanics: Non-Relativistic Theory* (Fizmatlit, Moscow, 2004).